

# The FLARE™ Intraoperative Near-Infrared Fluorescence Imaging System: A First-in-Human Clinical Trial in Breast Cancer Sentinel Lymph Node Mapping

Susan L. Troyan, MD<sup>1</sup>, Vida Kianzad, PhD<sup>2</sup>, Summer L. Gibbs-Strauss, PhD<sup>2</sup>, Sylvain Gioux, MEng<sup>2</sup>, Aya Matsui, MD, PhD<sup>2</sup>, Rafiou Oketokoun, MEng<sup>2,3</sup>, Long Ngo, PhD<sup>4</sup>, Ali Khamene, PhD<sup>3</sup>, Fred Azar, PhD<sup>3</sup>, and John V. Frangioni, MD, PhD<sup>2,5</sup>

<sup>1</sup>Breast Care Center, Department of Surgery, Beth Israel Deaconess Medical Center, Boston, MA; <sup>2</sup>Division of Hematology/Oncology, Department of Medicine, Beth Israel Deaconess Medical Center, Boston, MA; <sup>3</sup>Siemens Corporate Research, Princeton, NJ; <sup>4</sup>Division of General Medicine, Department of Medicine, Beth Israel Deaconess Medical Center, Boston, MA; <sup>5</sup>Department of Radiology, Beth Israel Deaconess Medical Center, Boston, MA

## ABSTRACT

**Background.** Invisible NIR fluorescent light can provide high sensitivity, high-resolution, and real-time image-guidance during oncologic surgery, but imaging systems that are presently available do not display this invisible light in the context of surgical anatomy. The FLARE™ imaging system overcomes this major obstacle.

**Methods.** Color video was acquired simultaneously, and in real-time, along with two independent channels of NIR fluorescence. Grayscale NIR fluorescence images were converted to visible “pseudo-colors” and overlaid onto the color video image. Yorkshire pigs weighing 35 kg (n = 5) were used for final preclinical validation of the imaging system. A six-patient pilot study was conducted in women undergoing sentinel lymph node (SLN) mapping for breast cancer. Subjects received <sup>99m</sup>Tc-sulfur colloid lymphoscintigraphy. In addition, 12.5 µg of indocyanine green (ICG) diluted in human serum albumin (HSA) was used as an NIR fluorescent lymphatic tracer.

**Results.** The FLARE™ system permitted facile positioning in the operating room. NIR light did not change the look of the surgical field. Simultaneous pan-lymphatic and SLN mapping was demonstrated in swine using clinically available NIR fluorophores and the dual NIR capabilities of the system. In the pilot clinical trial, a total of nine SLNs were

identified by <sup>99m</sup>Tc- lymphoscintigraphy and nine SLNs were identified by NIR fluorescence, although results differed in two patients. No adverse events were encountered. **Conclusions.** We describe the successful clinical translation of a new NIR fluorescence imaging system for image-guided oncologic surgery.

Presently, ultrasound and x-ray fluoroscopy are the two imaging techniques most utilized during human surgery. However, ultrasound requires direct contact with tissue and only sees a thin “slice” of the surgical field-of-view (FOV), and x-ray fluoroscopy exposes patients and caregivers to ionizing radiation. Importantly, neither technique is amenable to targeted contrast agents, which are a requirement for many procedures, such as image-guidance oncologic surgery (reviewed by Frangioni).<sup>1</sup>

Near-infrared (NIR) light, in the wavelength range of 700 to 900 nm, offers several significant advantages over presently available imaging techniques, including relatively high photon penetration into, and out of, living tissue, due to reduced absorbance and scatter, and a relatively high signal-to-background ratio (SBR) due to low tissue autofluorescence (reviewed by Frangioni).<sup>2</sup> However, NIR light is invisible to the human eye, so special optical imaging systems are required to “see” it on the surgical field. A NIR fluorophore is a chemical compound that converts NIR light of one wavelength into NIR light of a different wavelength. By shining high-intensity, invisible NIR light of one wavelength onto the surgical field, and detecting invisible NIR light of this different wavelength, the exact location of the NIR fluorophore can be determined. By targeting the NIR

fluorophore to a particular lumen, tissue, or organ, invisible NIR fluorescent light can be used to “see” any desired structure, or structures, on the surgical field. NIR fluorescent light has already been used clinically by several groups for sentinel lymph node (SLN) mapping in breast cancer, gastric cancer, and colon cancer by using indocyanine green (ICG) as the lymphatic tracer.<sup>3–8</sup> None of these studies, however, was able to visualize invisible NIR fluorescence in the context of surgical anatomy, or used an ICG formulation optimized for clinical use.

In 2002 our laboratory introduced the first prototype of a surgical imaging system that could acquire color video and NIR fluorescence emission simultaneously and in real-time.<sup>9</sup> The features of this system included acquisition of NIR fluorescence emission in the context of surgical anatomy (i.e., provided by the color video camera) and no change to the look of the surgical field, because NIR light is invisible. This so-called FLARE™ (Fluorescence-Assisted Resection and Exploration) surgical imaging system underwent considerable refinements over the years, including compatibility with large animal surgery, the addition of hands-free operation, introduction of more compact optics, development of a software system capable of live and simultaneous 30 frames-per-second (fps) multi-camera acquisition, and most recently, introduction of the type of high-power, multi-channel, computer-controlled LED light source required for human surgery.<sup>10–13</sup> To date, the FLARE™ imaging system has been validated in more than 200 rodent and 100 large animal surgeries.<sup>9,10,12,14–42</sup>

This study describes the results from a multiyear Bioengineering Partnership (BRP) grant from the National Institutes of Health (NIH) designed to translate the technology to the clinic, and a NIH R21 Quick Trials in Imaging grant designed for first-in-human testing of the FLARE™ imaging system in women undergoing SLN mapping for breast cancer.

## METHODS

### *Preparation of NIR Fluorophores*

Methylene blue injection USP (1%; 10 mg/ml) was purchased from Taylor Pharmaceuticals (Buffalo Grove, IL), diluted into 10 ml of saline, and injected intravenously as a bolus at a dose of 1 mg/kg. Indocyanine green (ICG) USP (25-mg vials) was purchased from Akorn (Decatur, IL) and resuspended in 10 ml of supplied diluent to yield a 2.5 mg/ml (3.2 mM) stock solution; 0.16 ml of this ICG stock solution was then transferred to a 50-ml bag of Buminat (25% human serum albumin [HSA] solution; Baxter Healthcare, Deerfield, IL) to yield 10 µM ICG in HSA (ICG:HSA).

### *FLARE™ Imaging System Components*

The portable cart and articulating arm were from Yankee Modern Engineering (Groton, MA). The satellite monitor stand was from GCX (Petaluma, CA). Ultra-sharp DVI monitors (20”) were from Dell (Round Rock, TX). The imaging head, comprised of a high-power, computer-controlled LED light housing, custom optics, custom filtration, and cameras, has been described in detail previously, as has the foot switch control for the system.<sup>11,13</sup> Hardware was engineered to meet all relevant subsections of the Association for the Advancement of Medical Instrumentation (AAMI)/International Electrotechnical Commission (IEC) standard #60601. A customized software system using the NIH-developed Extensible Imaging Platform (XIP) enabled control of the hardware, and permitted simultaneous acquisition of images from a color video camera and two NIR fluorescence cameras at up to 30 fps.<sup>43</sup> The software also permitted each grayscale NIR image to be “pseudo-colored” from a palette of more than 256 visible colors and overlaid in real-time onto the color video image. For intraoperative use, a 0.118”-thick acrylic splash shield having 95% optical transmission at 800 nm was hermetically bonded to a clear plastic drape and sterilized (Medical Technique, Inc., Tucson, AZ). Using sterile technique, the shield was inserted into the bottom of the imaging head, and the drape unwrapped up, and over, the entire system. Additional details can be found at [www.frangionilab.org](http://www.frangionilab.org). Separate, dedicated FLARE™ systems were used for animal and human surgery.

### *Animal Model Systems*

Animals ( $n = 5$ ) were studied under the supervision of an approved institutional protocol. Female Yorkshire pigs (E. M. Parsons and Sons, Hadley, MA) averaged 35 kg. Pigs were induced with 4.4 mg/kg intramuscular Telazol (Fort Dodge Labs, Fort Dodge, IA), intubated, and maintained with 2% isoflurane (Baxter Healthcare, Deerfield, IL). Vital signs were monitored continuously. Excitation fluence rate for white light, 700 nm excitation light, and 800 nm excitation light were 20,000 lux, 2 mW/cm<sup>2</sup>, and 8 mW/cm<sup>2</sup>, respectively.

### *First-in-Human Clinical Trial*

The clinical trial was approved by the Institutional Review Board (IRB) of the Beth Israel Deaconess Medical Center and was performed in accordance with the ethical standards of the Helsinki Declaration of 1975. The IRB deemed the FLARE™ imaging system a “non-significant risk” device. All patients gave informed consent and were

anonymized. Clinical trial participants were women undergoing SLN mapping for breast cancer. All subjects received the standard-of-care with injection, on average, of 834  $\mu\text{Ci}$   $^{99\text{m}}\text{Tc}$ -sulfur colloid performed by the covering nuclear medicine physician approximately 2 hours before surgery.  $^{99\text{m}}\text{Tc}$ -sulfur colloid was administered as four deep peritumoral injections and four subcutaneous peritumoral injections of  $\approx 0.2$  ml each. In the operating room, a single surgeon (Dr. Troyan) injected a total of 1.6 ml of ICG:HSA, given as four deep peritumoral injections and four subcutaneous peritumoral injections of  $\approx 0.2$  ml each. The injection site was massaged for approximately 5 minutes. Lymphatic mapping using a handheld gamma probe was performed as per standard practice except that the 40,000 lux of white (400–650 nm) light illuminating the surgical field was provided by the FLARE™ imaging system, which was positioned 18" away from the patient. Settings included 14  $\text{mW}/\text{cm}^2$  of 760 nm NIR fluorescence excitation light, a 67 msec color video camera exposure time, and a 67 to 250 msec 800 nm NIR fluorescence camera exposure time.

## RESULTS

### Design of the FLARE™ Imaging System

In consultation with practicing surgeons, it became apparent that a general-purpose optical imaging system for surgery must: 1) show the invisible NIR fluorescent light in the context of surgical anatomy, i.e., overlaid onto the color video image; and 2) provide two independent channels of NIR fluorescent light for procedures that, for example, require resection of one tissue (such as a tumor) as well as avoidance of other tissues (such as nerves and blood vessels). These design criteria were satisfied using the optical imaging system components shown in Fig. 1a. By paying careful attention to light filtration, and by using dichroic mirrors to direct light to a color video camera or two different NIR cameras (Fig. 1b), the FLARE™ imaging head is capable of simultaneous, real-time image acquisition from all three cameras.<sup>13</sup> Detailed specifications of the FLARE™ imaging system are provided in Table 1, and include an adjustable FOV from 2.2 to 15 cm, a resolution of 125 to 625  $\mu\text{m}$ , and an 18" working distance between the imaging head and the patient. A graphical user interface included with the software provides simple, point-and-click control of the system.

### Deployment in the Operating Room

The FLARE™ imaging system is built on a portable cart designed to withstand up to 10° of tilt. The cart houses two

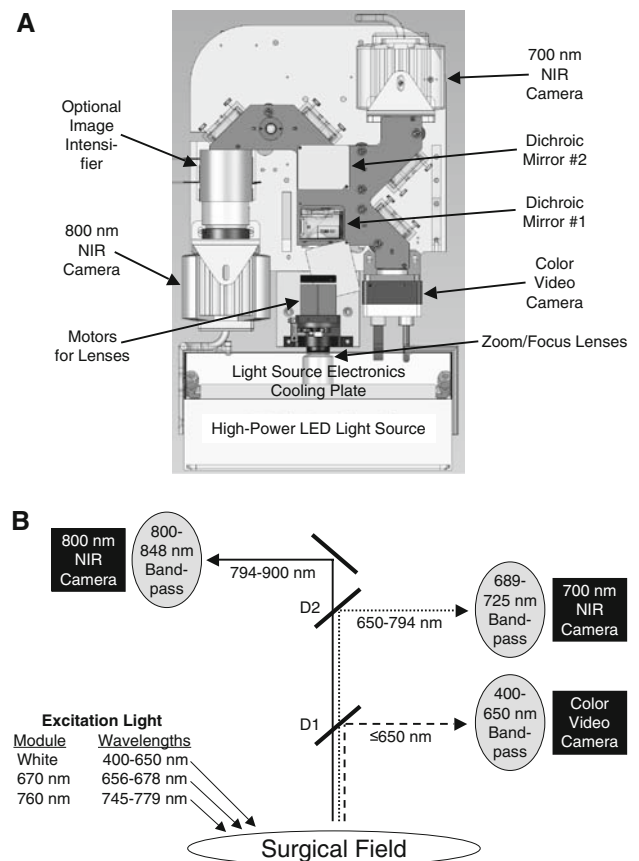


**FIG. 1** FLARE™ Near-Infrared Fluorescence Imaging System. **a** Detailed schematic of imaging head. **b** Optical light paths and filtration for the FLARE™ imaging system having a color video camera, and two independent and simultaneous NIR cameras (700 nm emission and 800 nm emission). D1 = 680 nm dichroic mirror. D2 = 770 nm dichroic mirror

monitors for the technologist operating the system. One monitor displays control software, and the other displays a duplicate of the surgeon's monitor. The surgeon's monitor is on a satellite pole, which can be positioned in any convenient location up to 16 feet from the cart. Deployment of the system in the operating room where the clinical trial described below was conducted is shown in Fig. 2a.

Attached to the cart is a specially designed 6 degree-of-freedom (DOF) articulated arm. Depression of either one of the two brake release buttons on the imaging head handles releases the arm brakes and permits smooth and precise positioning of the imaging head over the surgical field (Fig. 2b). Release of the button engages the brakes and fixes the location of the imaging head in three-dimensional space. The overall reach of the articulated arm is 43–70" from the floor and up to 50.7" from cart.

Hands-free operation of the FLARE™ imaging system is accomplished using a 6-pedal foot switch (not shown), which can be configured for any software functions. For this study, the foot switch was programmed for zoom-in

**TABLE 1** FLARE™ Imaging System Specifications

Category	Specification	Description
Physical	Size	Mobile cart: 32" W x 32" D x 41.4" H; Mast height: 82"
	Weight	675 lb, including all electronics
	Arm	6 degree-of-freedom; Reach: 43–70" from floor, 50.7" from cart
Electrical	Voltage and plug	120 V AC, 60 Hz; single NEMA 5-15 120 V/15 A AC plug
	Current	15 A max
	Grounding	Isolation transformer for all components; redundant chassis grounding
	Leakage current	<300 $\mu$ A (per AAMI/IEC #60601)
Sterility	Shield	Disposable acrylic shield with $\geq$ 95% transmission
	Drape	Disposable, custom-fit plastic drape bonded to shield
Light source	Housing	Anodized aluminum with secondary 400-W cooling plate
	Elements	Custom 25-mm circular LED arrays w/ integrated linear drivers
	Electronics	Custom passive and active boards with embedded controller
	Fluence rates	40,000 lux white light (400–650 nm), 4 mW/cm <sup>2</sup> of 700 nm (656–678 nm) excitation light, 14 mW/cm <sup>2</sup> of 800 nm (745–779 nm) excitation light
Optics	Working distance	18" (45 cm) from surface of patient
	Field-of-view	2.2 W x 1.7 H cm to 15 W x 11.3 cm (adjustable zoom)
	Emission/reflectance Channels	Color video (400–650 nm), 700 nm fluorescence (689–725 nm), 800 nm fluorescence (800–848 nm), all with simultaneous acquisition
	Pixel resolution	640 x 480 for each camera
	System resolution	125 x 125 $\mu$ m (x,y) to 625 x 625 $\mu$ m (x,y)
	Display refresh	Up to 15 Hz simultaneous acquisition on all 3 cameras
	NIR exposure time	Adjustable from 100 $\mu$ sec to 8 sec
Hands-free	Optics	Automatic zoom/focus
	Control	6-pedal foot switch
Monitors	Number	2 cart-mounted 20" for operator; 1 satellite 20" on stand for surgeon

(with auto-focus), zoom-out (with auto-focus), single-shot image acquire, single-shot image recall, cine (movie) save, and cine (movie) recall.

Imaging system sterility was achieved with a sterile splash shield/drape combination, which could be applied in the operating room using sterile technique, and which covered the imaging head, articulated arm, and cart.<sup>13</sup>

#### Final Preclinical Validation

Human clinical trials that use NIR fluorescence imaging are currently constrained by the fact that there are only two clinically available NIR fluorophores: methylene blue (MB) and ICG<sup>42</sup>; neither is presently FDA-approved for lymph node mapping. Fortunately, these agents fluoresce at different NIR wavelengths, with MB having peak emission in the 700-nm range and ICG in the 800-nm range. MB and ICG thus provide the means to test the full capabilities of the FLARE™ imaging system under realistic clinical conditions.

Previously, we have demonstrated that ICG alone was a nonoptimal agent for SLN mapping, due to its relatively

low quantum yield (QY) and small hydrodynamic diameter (HD).<sup>36</sup> The relatively low QY results in decreased brightness of the NIR fluorescence signal, and the small HD results in ICG flowing through the SLN into second-tier nodes. However, simple incubation of ICG with human serum albumin (HSA) resulted in a 1:1 complex (ICG:HSA), which had a threefold higher QY, and a HD of  $\approx$ 7 nm, which improves SLN retention.<sup>36</sup>

To complete preclinical validation of the FLARE™ imaging system for lymph node mapping, Yorkshire pigs approaching the size of humans were injected intravenously with 1 mg/kg of MB followed by injection of the colon parenchyma with 10  $\mu$ g of ICG:HSA, prepared as described in *Materials and Methods*. In unpublished work, we have found that intravenously injected MB is excreted into bile but then reabsorbed by the intestine, resulting in very bright 700 nm NIR fluorescence of all mesenteric lymph nodes. Thus, MB can be used to visualize all lymph nodes of the mesentery, whereas ICG:HSA can be used to identify which node is the SLN. As shown in Fig. 3, the dual NIR capabilities of the FLARE™ imaging system permitted sensitive, real-time identification of all lymph

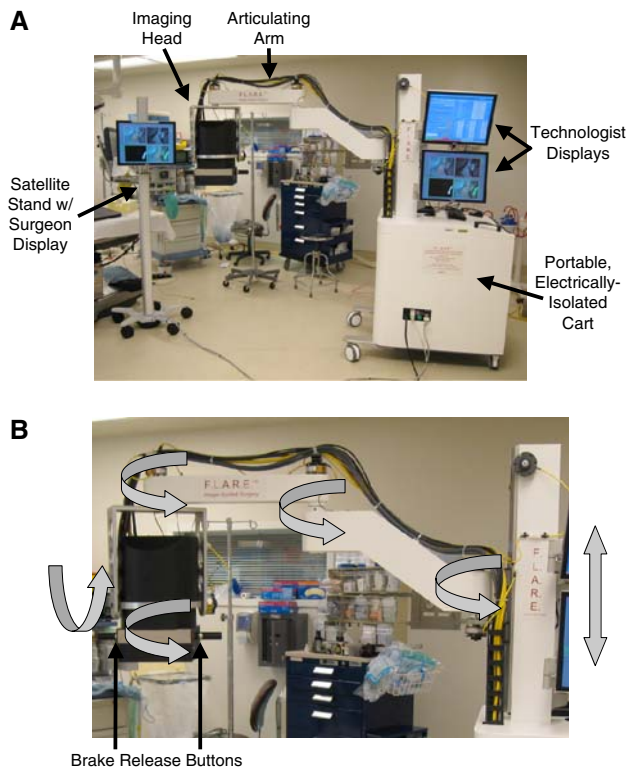


**FIG. 2** Deployment in the operating room and range of motion. **a** Portable imaging system and satellite monitor stand deployed in the operating room. Foot switch not shown. **b** Six degrees-of-freedom range of motion (gray arrows) and brake release buttons of the imaging head

nodes present in the surgical field, as well as definitive identification of the SLN. Importantly, the “pseudo-color” and overlay features of the software permitted color-coding of each type of node, with all nodes being displayed in red, the SLN and its lymphatic channels being displayed in green, and overlap of the two colors appearing as yellow (Fig. 3).

#### First-in-Human Clinical Trial

After IRB approval, a 6-patient clinical trial of the FLARE™ imaging system was conducted in women undergoing SLN mapping for breast cancer. All patients provided informed consent and received the standard-of-care with  $^{99m}\text{Tc}$ -sulfur colloid lymphoscintigraphy as described in *Materials and Methods*. Subjects also received intratumoral/subcutaneous injection of ICG:HSA in the operating room, followed by massage of the site for 5 minutes. The FLARE™ imaging system was used to image the surgical field before, during, and after ICG:HSA injection. Because NIR light is invisible, there was no change to the look of the surgical field. On the monitor, however, the surgeon was able to visualize the injection,

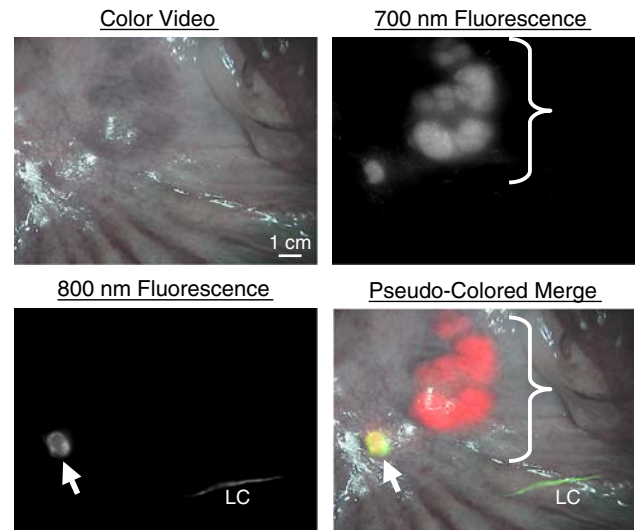


**FIG. 3** Simultaneous, NIR fluorescent pan-lymph node mapping and sentinel lymph node mapping in swine. All lymph nodes of the mesentery (bracket) fluoresce at 700 nm (pseudo-colored red) after a single intravenous injection of 1 mg/kg of methylene blue. SLN (arrow) fluorescing at 800 nm (pseudo-colored green) is identified after intraparenchymal injection of 10  $\mu\text{M}$  of ICG:HSA into the colon wall, and appears yellow. The lymphatic channel (LC) feeding the SLN appears green. All camera exposure times were 67 msec. Data are representative of  $n = 5$  pigs

lymphatic flow, and retention of ICG:HSA and could use the color-NIR merged image to exactly pinpoint the lymph node of interest.

The clinical characteristics of all patients are provided in Table 2, and typical results from intraoperative imaging are shown in Fig. 4. Patient 1 was an interesting case, in whom three SLNs were identified using conventional  $^{99m}\text{Tc}$ -sulfur colloid lymphoscintigraphy but four SLNs were identified using NIR fluorescence (Fig. 4a). The radioactive counts of the fourth SLN, seen by NIR fluorescence but not lymphoscintigraphy, were no higher than background. Importantly, this fourth lymph node had macroscopic breast cancer metastases (Table 2).

In four of six patients, the SLNs identified by lymphoscintigraphy were the same as those identified by NIR fluorescence. In patient 6, two SLNs were identified by lymphoscintigraphy and only one by NIR fluorescence. Overall, a total of nine SLNs in six patients were identified by  $^{99m}\text{Tc}$ -sulfur colloid lymphoscintigraphy, and nine SLNs were identified by NIR fluorescence.

The real-time and high-resolution features of the FLARE™ imaging system are highlighted in Fig. 4b using the data from Patient 2. In this case, lymphatic flow deep within the axilla could be visualized and, during SLN resection, there was unambiguous discrimination of the SLN from surrounding non-SLNs.

TABLE 2 Patient characteristics, identification of SLNs, and pathology results

Patient	Age (yr)	Height (ft)	Weight (lb)	Body mass index	Skin type	Location of primary tumor	Size of primary tumor (cm)	Histological type	Histological grade	Node number	Node identified using radioactivity	Node identified using NIR fluorescence	Node histology	Axillary node dissection (Pos/Tot)
1	65	5'1"	160	30.2	I	Lt; UO	1.3	ILC	II	1	Yes	Yes	-	0/6
2	62	5'7"	230	36.0	III	Rt; UO	0.9	IDC	I	1	Yes	Yes	-	n.d.
3	64	5'4"	178	30.6	II	Lt; IC	1.8	IMPC	II/III	1	Yes	Yes	m	0/11
4	51	5'4"	152	26.1	III	Rt; UC	0.7	IDC	I	1	Yes	Yes	-	n.d.
5	65	5'7"	187	29.3	III	Lt; LO	0.9	IDC	III	1	Yes	Yes	-	n.d.
6	60	5'4"	160	27.5	II	Lt; UC	1	IDC	II	1	Yes	No	-	n.d.
<b>Totals</b>										<b>9</b>	<b>9</b>	<b>9</b>		

Skin type = American Academy of Dermatology Skin Types I-VI:

I. Pale, white skin: always burns easily; never tans (Celtic, Scandinavian, and infants)

II. White: usually burns easily; tans minimally (Northern European)

III. White (average): sometimes burns; tans gradually to light brown (Central European)

IV. Beige or lightly tanned: burns minimally; always tans to moderately brown (Mediterranean, Asian)

V. Moderate brown or tanned: rarely burns; tans well (South American, Indian, Native American)

VI. Dark brown or black: never burns; deeply pigmented (African, African-American, Aborigine)

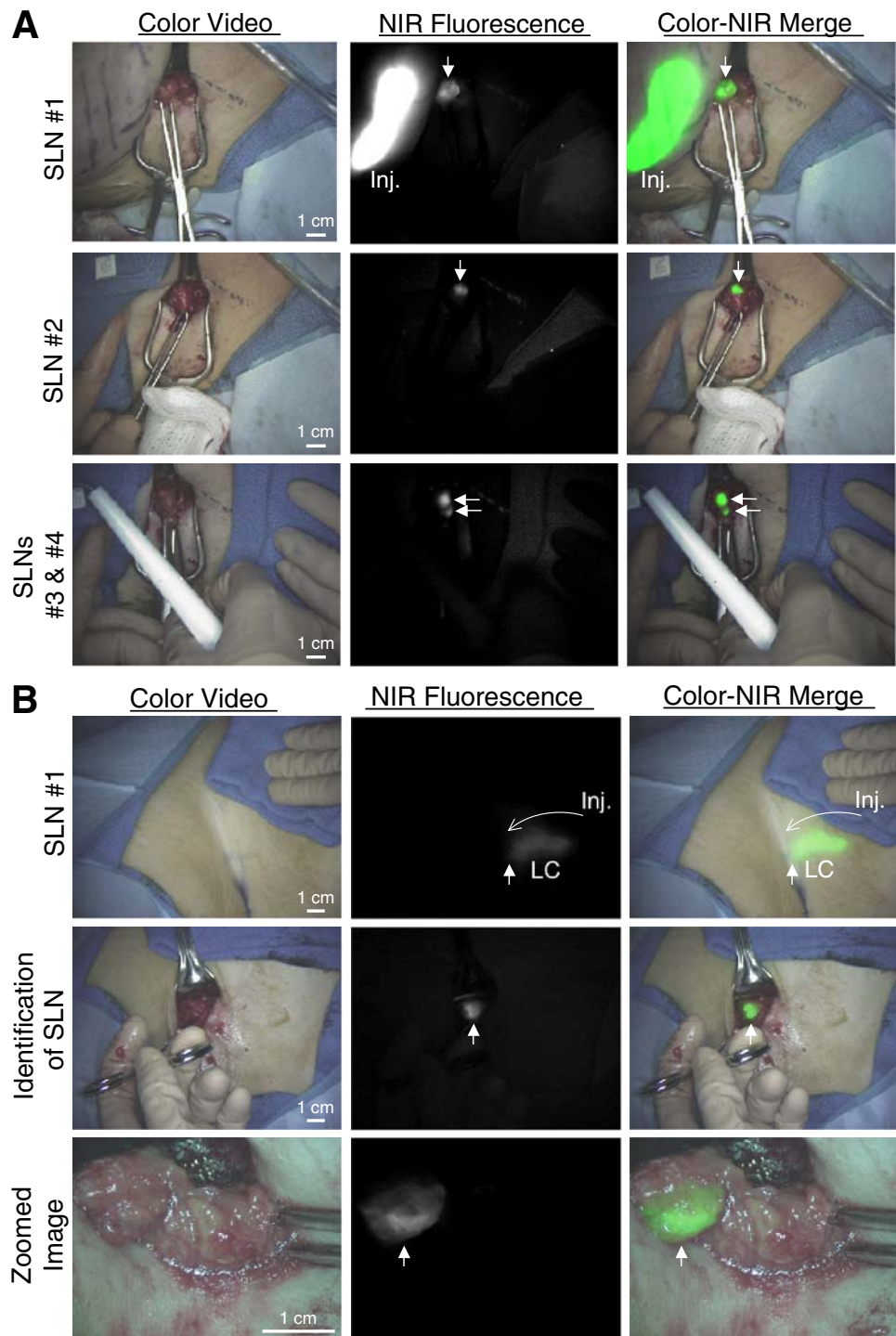
Location of primary tumor: Lt = left; Rt = right; C = center; I = inner; L = lower; O = outer; U = upper

Histological types: IDC = invasive ductal carcinoma; ILC = intralobular carcinoma; IMPC = invasive micropapillary carcinoma

Node histology: - = no evidence of metastasis; m = micrometastases <1 mm; + = metastases  $\geq$  1 mm

Axillary node dissection: Pos = number of positive lymph nodes identified; Tot = total lymph nodes identified; n.d. = not done

**FIG. 4** NIR fluorescent sentinel lymph node mapping in women with breast cancer. Shown are color video images (*left*), 800 nm NIR fluorescence images (*middle*), and a pseudocolored (*lime green*) merge of the two (*right*) after injection (Inj.) of 10  $\mu$ M ICG:HSA. **a** Four SLNs (*arrows*) identified and resected for Patient #1. 800-nm camera exposure time was 200 msec. **b** Single SLN identified and resected for Patient #2. Shown are flow through a lymphatic channel (LC) and position of the SLN (*arrow*; *top row*), identification of the SLN (*arrow*; *middle row*), and a zoomed image of the SLN (*arrow*) during resection (*bottom row*). Note multiple non-SLNs nearby. 800-nm camera exposure time was 200 msec



## DISCUSSION

NIR fluorescence-guided surgery requires optimized imaging systems and optimized NIR fluorescent contrast agents. In this study, we described an optical imaging system that was designed based on the needs of surgeons, and with ergonomics amenable to the operating room. The system is completely portable, electrically isolated for

safety, provides facile positioning over the patient, is noncontact (18" working distance), and provides micron-resolution over a large FOV.

The key feature of the FLARE™ imaging system is its ability to see color video images (i.e., surgical anatomy) simultaneously with two independent channels of NIR fluorescence. The importance of dual NIR capability is highlighted in Fig. 3; one can imagine how these two NIR

channels (700 nm and 800 nm) could be exploited for any surgical procedure. During cancer surgery, for example, one NIR channel could be reserved for resection of the tumor and the other for avoidance of nerves. During vascular surgery, one NIR channel could be reserved for detection of intravascular thrombi and the other for vascular patency or anastomotic leak.<sup>10,41,42</sup> During general surgery, one channel could be reserved for identification of lumens, such as the bile ducts or ureters, and the other for the location of blood vessels or nerves.<sup>10,28,39,41</sup> Many future applications of the FLARE™ technology, however, will require development of contrast agents for specific applications.

ICG:HSA is a reasonable, short-term solution as a lymphatic tracer for SLN mapping using NIR fluorescence, although it is not ideal with respect to optical properties or SLN retention. It does, however, offer significant advantages over small molecule lymphatic tracers, such as MB and ICG, including a larger hydrodynamic diameter, resulting in better SLN retention, high fluorescence quantum yield (i.e., brightness), and high contrast using NIR fluorescence rather than blue color.<sup>36</sup> It is difficult to predict whether the addition of a small molecule blue dye, such as isosulfan blue or MB, to <sup>99m</sup>Tc-sulfur colloid lymphoscintigraphy would have improved detection of lymph node #4 from Patient 1, because the injection technique (discussed below) was an uncontrolled variable in our study.<sup>44</sup> Fortunately, contrast agent development is progressing rapidly in both academia and industry, and it is expected that optimal NIR fluorescent lymphatic tracers for SLN mapping will soon be available.

The present incarnation of the FLARE™ imaging system is not without limitations. The surgeon conducting this study preferred the imaging head to be 90° relative to the floor, facing directly into the axilla. Such an angle would be better served by a smaller, more compact imaging head. Although NIR fluorescence excitation fluence rate (i.e., brightness) was adequate to pinpoint SLNs that were several centimeters deep in the axilla, a higher fluence rate would have permitted shorter NIR camera acquisition times. Previously, we have defined the photobleaching threshold for NIR fluorophores of the heptamethine indocyanine class.<sup>18,23</sup> In general, fluence rate should be kept to  $\leq 50$  mW/cm<sup>2</sup>, which means that the present FLARE™ imaging system, having a 14 mW/cm<sup>2</sup> fluence rate for 760 nm excitation light, could be  $\approx 3.5$ -fold brighter without risk of photobleaching. Marks drawn on the skin with many brands of surgical markers were NIR fluorescent. This interfered with the ability to see draining lymphatics. Because conventional operating room lights produce significant amounts of NIR light, white light illuminating the surgical field must be provided by the FLARE™ system, and all other operating room lights need

to be dim or off. The NIR excitation light for the 700 nm emission channel will tend to “tinge” the surgical field in a reddish hue unless it is properly balanced with white light. Finally, a minimally invasive (laparoscopy) version of the FLARE™ imaging system will be needed for many non-open surgeries, and such a system is under active development.

In this era of concern about healthcare costs, a transparent discussion of the costs associated with FLARE™ technology is warranted. The current version of the FLARE™ system is comprised of parts totaling approximately \$120,000 USD. When purchased in quantity, and assembled using modern manufacturing techniques, the true cost of the system will be a much smaller fraction of this amount. The ICG:HSA lymphatic tracer used in this study costs approximately \$109 per patient, comprised of \$73 for the ICG and \$36 for the HSA. These costs should be considered in the context of <sup>99m</sup>Tc-sulfur colloid lymphoscintigraphy. A handheld gamma probe system for SLN mapping costs approximately \$20,000, and a dose of <sup>99m</sup>Tc-sulfur colloid costs approximately \$32 per patient. Because costs associated with <sup>99m</sup>Tc-sulfur colloid lymphoscintigraphy have been relatively stable, it is probable that NIR fluorescence technology could become competitive as commercialization occurs and costs fall. Indeed, our laboratory has already developed the “Mini-FLARE™” version of the system (manuscript in preparation), which reduces costs to be competitive with conventional lymphoscintigraphy. The tangible advantages of NIR fluorescence also must be considered. NIR fluorescence provides true two-dimensional imaging rather than point-probing, is real-time, helps remove ambiguity associated with SLN detection, could ultimately save considerable operating room time, could eliminate the need for both a nuclear medicine physician and injection of ionizing radiation, and guides the pathologist to precise location within the node (i.e., sinus entry site) that is most likely to harbor metastases.

The first-in-human trial of the system confirmed several observations made during previously published rodent and swine lymphatic mapping studies.<sup>12,16,18,19,25,27,31–34,36,40</sup> First, NIR light did not change the look of the surgical field, so the learning curve for using the technology was minimal. Second, NIR fluorescence could be used to see lymphatic flow and to pinpoint the general location of the SLN even before an incision is made. The body habitus of the six patients differed over a wide range, resulting in SLNs as deep as 4 cm from the surface, and yet SLN identification was still possible. Skin types in these trial subjects only ranged from types I to III. Darker skin is not expected to cause significant problems, because pigmentation is restricted to such a thin layer ( $\approx 1$  mm); however, this must be tested formally in subjects with type VI skin. Finally, NIR fluorescence was able to unambiguously



identify SLNs, even when part of a larger cluster of surrounding lymph nodes.

We caution over-interpreting the SLN identification results from this pilot trial. On one hand, the sensitivity of NIR fluorescence detection, using radioactive detection as the “gold standard,” was 100% (9 SLNs identified by both techniques). However, the two lymphatic tracers,  $^{99m}\text{Tc}$ -sulfur colloid and ICG:HSA, were injected by different clinicians 2 hours apart, with no control over injection location or depth. Thus, it is possible that different lymph node territories were being interrogated. This asynchrony in time was necessary because  $^{99m}\text{Tc}$ -sulfur colloid has a large HD and requires a long migration time to reach the SLN. On the contrary, ICG:HSA requires only  $\approx 5$  minutes to reach the SLN. The NIR fluorescence signal in the SLN is lower at 30 minutes, and because the HD of ICG:HSA is only intermediate ( $\approx 7$  nm), it is not advisable to wait longer than 30 minutes to complete the procedure. In future studies, the same clinician will perform radioactive and NIR fluorescent lymphatic tracer injections, which may help reduce variability in the number of SLNs identified. Of note, we saw no evidence of second-tier lymph nodes being labeled by ICG:HSA in the 5 to 30 minutes in which the mapping procedure was completed.

In summary, the FLARE™ image-guided surgery system has been successfully translated from preclinical studies to clinical studies and is now poised for further evaluation in a variety of human surgeries.

**ACKNOWLEDGMENT** We thank Barbara L. Clough and Mir-eille Rosenberg for clinical trial preparation, Judith Hirshfield-Bartek for assistance with patient medical histories, Eiichi Tanaka, M.D. for preliminary swine studies, and Sunil Gupta and Razvan Ciocan for technical assistance with the imaging system. This study was supported by the following grants from the National Institutes of Health (National Cancer Institute) to JVF: Bioengineering Research Partnership grant #R01-CA-115296 and Quick Trials for Imaging grant #R21-CA-130297. We thank the following individuals and companies for their contributions to this project: Gordon Row (Yankee Modern Engineering), Kelly Stockwell and Paul Millman (Chroma Technology), David Comeau and Robert Waitt (Albright Technologies), Gary Avery, Phil Dillon, and Ed Schultz (Qioptiq Imaging Solutions), Jeffrey Thumm (Duke River Engineering), Michael Paszak and Victor Laronga (Microvideo Instruments), Colin Johnson (LAE Technologies), Robert Eastlund (Graftek Imaging), John Fortini (Lauzon Manufacturing), Steve Huchro (Solid State Cooling), Clay Sakewitz and Will Richards (Design and Assembly Concepts), Ken Thomas and Fernando Irizarry (Sure Design), Paul Bistline and Phil Bonnette (Medical Technique, Inc.), Mathew Silverstein (L-com), and Jim Cuthbertson (Nashua Circuits).

**FINANCIAL DISCLOSURE** This study was supported by the following grants from the National Institutes of Health (National Cancer Institute) to JVF: Bioengineering Research Partnership grant #R01-CA-115296 and Quick Trials for Imaging grant #R21-CA-130297. All intellectual property associated with the FLARE™ imaging system is owned by the Beth Israel Deaconess Medical Center, which has licensed it nonexclusively to GE Healthcare. As inventor of the technology, Dr. Frangioni may someday receive

royalties if a product is commercialized. No other authors have any financial interest in this study.

## REFERENCES

1. Frangioni JV. New technologies for human cancer imaging. *J Clin Oncol*. 2008;26:4012–21.
2. Frangioni JV. In vivo near-infrared fluorescence imaging. *Curr Opin Chem Biol*. 2003;7:626–34.
3. Fujiwara M, Mizukami T, Suzuki A, Fukamizu H. Sentinel lymph node detection in skin cancer patients using real-time fluorescence navigation with indocyanine green: preliminary experience. *J Plast Reconstr Aesthet Surg*. 2008 [Epub ahead of print].
4. Kitai T, Inomoto T, Miwa M, Shikayama T. Fluorescence navigation with indocyanine green for detecting sentinel lymph nodes in breast cancer. *Breast Cancer*. 2005;12:211–5.
5. Ogasawara Y, Ikeda H, Takahashi M, Kawasaki K, Doihara H. Evaluation of breast lymphatic pathways with indocyanine green fluorescence imaging in patients with breast cancer. *World J Surg*. 2008;32:1924–9.
6. Sevick-Muraca EM, Sharma R, Rasmussen JC, et al. Imaging of lymph flow in breast cancer patients after microdose administration of a near-infrared fluorophore: feasibility study. *Radiology*. 2008;246:734–41.
7. Kusano M, Tajima Y, Yamazaki K, Kato M, Watanabe M, Miwa M. Sentinel node mapping guided by indocyanine green fluorescence imaging: a new method for sentinel node navigation surgery in gastrointestinal cancer. *Dig Surg*. 2008;25:103–8.
8. Miyashiro I, Miyoshi N, Hiratsuka M, et al. Detection of sentinel node in gastric cancer surgery by indocyanine green fluorescence imaging: comparison with infrared imaging. *Ann Surg Oncol*. 2008;15:1640–3.
9. Nakayama A, del Monte F, Hajar RJ, Frangioni JV. Functional near-infrared fluorescence imaging for cardiac surgery and targeted gene therapy. *Mol Imaging*. 2002;1:365–77.
10. De Grand AM, Frangioni JV. An operational near-infrared fluorescence imaging system prototype for large animal surgery. *Technol Cancer Res Treat*. 2003;2:553–62.
11. Gioux S, De Grand AM, Lee DS, Yazdanfar S, Idoine JD, Lomnes SJ, Frangioni JV. Improved optical sub-systems for intraoperative near-infrared fluorescence imaging. *SPIE Proc*. 2005;6009:39–48.
12. Tanaka E, Choi HS, Fujii H, Bawendi MG, Frangioni JV. Image-guided oncologic surgery using invisible light: completed pre-clinical development for sentinel lymph node mapping. *Ann Surg Oncol*. 2006;13:1671–81.
13. Gioux S, Kianzad V, Ciocan R, Gupta S, Oketokoun R, Frangioni JV. High power, computer-controlled, LED-based light sources for fluorescence imaging and image-guided surgery. *Mol Imaging*. 2009 (in press).
14. Bhushan KR, Misra P, Liu F, Mathur S, Lenkinski RE, Frangioni JV. Detection of breast cancer microcalcifications using a dual-modality SPECT/NIR fluorescent probe. *J Am Chem Soc*. 2008;130:17648–9.
15. Choi HS, Liu W, Misra P, et al. Renal clearance of quantum dots. *Nat Biotechnol*. 2007;25:1165–70.
16. Frangioni JV, Kim SW, Ohnishi S, Kim S, Bawendi MG. Sentinel lymph node mapping with type-II quantum dots. *Methods Mol Biol*. 2007;374:147–59.
17. Humblet V, Lapidus R, Williams LR, et al. High-affinity near-infrared fluorescent small-molecule contrast agents for in vivo imaging of prostate-specific membrane antigen. *Mol Imaging*. 2005;4:448–62.

18. Kim S, Lim YT, Soltesz EG, et al. Near-infrared fluorescent type II quantum dots for sentinel lymph node mapping. *Nat Biotechnol.* 2004;22:93–7.
19. Kim SW, Zimmer JP, Ohnishi S, Tracy JB, Frangioni JV, Bawendi MG. Engineering InAs(x)P(1-x)/InP/ZnSe III-V alloyed core/shell quantum dots for the near-infrared. *J Am Chem Soc.* 2005;127:10526–32.
20. Lenkinski RE, Ahmed M, Zaheer A, Frangioni JV, Goldberg SN. Near-infrared fluorescence imaging of microcalcification in an animal model of breast cancer. *Acad Radiol.* 2003;10:1159–64.
21. Liu F, Bloch N, Bhushan KR, et al. Humoral bone morphogenetic protein 2 is sufficient for inducing breast cancer microcalcification. *Mol Imaging.* 2008;7:175–86.
22. Liu W, Choi HS, Zimmer JP, Tanaka E, Frangioni JV, Bawendi M. Compact cysteine-coated CdSe(ZnCdS) quantum dots for in vivo applications. *J Am Chem Soc.* 2007;129:14530–1.
23. Nakayama A, Bianco AC, Zhang CY, Lowell BB, Frangioni JV. Quantitation of brown adipose tissue perfusion in transgenic mice using near-infrared fluorescence imaging. *Mol Imaging.* 2003;2:37–49.
24. Ohnishi S, Vanderheyden JL, Tanaka E, et al. Intraoperative detection of cell injury and cell death with an 800 nm near-infrared fluorescent Annexin V derivative. *Am J Transplant.* 2006;6:2321–31.
25. Parungo CP, Colson YL, Kim SW, Kim S, Cohn LH, Bawendi MG, Frangioni JV. Sentinel lymph node mapping of the pleural space. *Chest.* 2005;127:1799–804.
26. Parungo CP, Ohnishi S, De Grand AM, et al. In vivo optical imaging of pleural space drainage to lymph nodes of prognostic significance. *Ann Surg Oncol.* 2004;11:1085–92.
27. Parungo CP, Soybel DI, Colson YL, et al. Lymphatic drainage of the peritoneal space: a pattern dependent on bowel lymphatics. *Ann Surg Oncol.* 2007;14:286–98.
28. Tanaka E, Ohnishi S, Laurence RG, Choi HS, Humblet V, Frangioni JV. Real-time intraoperative ureteral guidance using invisible near-infrared fluorescence. *J Urol.* 2007;178:2197–202.
29. Zaheer A, Lenkinski RE, Mahmood A, Jones AG, Cantley LC, Frangioni JV. In vivo near-infrared fluorescence imaging of osteoblastic activity. *Nat Biotechnol.* 2001;19:1148–54.
30. Zaheer A, Murshed M, De Grand AM, Morgan TG, Karsenty G, Frangioni JV. Optical imaging of hydroxyapatite in the calcified vasculature of transgenic animals. *Arterioscler Thromb Vasc Biol.* 2006;26:1132–6.
31. Zimmer JP, Kim SW, Ohnishi S, Tanaka E, Frangioni JV, Bawendi MG. Size series of small indium arsenide-zinc selenide core-shell nanocrystals and their application to in vivo imaging. *J Am Chem Soc.* 2006; 128:2526–7.
32. Soltesz EG, Kim S, Kim SW, et al. Sentinel lymph node mapping of the gastrointestinal tract by using invisible light. *Ann Surg Oncol.* 2006;13:386–96.
33. Parungo CP, Ohnishi S, Kim SW, et al. Intraoperative identification of esophageal sentinel lymph nodes with near-infrared fluorescence imaging. *J Thorac Cardiovasc Surg.* 2005;129:844–50.
34. Soltesz EG, Kim S, Laurence RG, et al. Intraoperative sentinel lymph node mapping of the lung using near-infrared fluorescent quantum dots. *Ann Thorac Surg.* 2005;79:269–77.
35. Ohnishi S, Garfein ES, Karp SJ, Frangioni JV. Radiolabeled and near-infrared fluorescent fibrinogen derivatives create a system for the identification and repair of obscure gastrointestinal bleeding. *Surgery.* 2006;140:785–92.
36. Ohnishi S, Lomnes SJ, Laurence RG, Gogbashian A, Mariani G, Frangioni JV. Organic alternatives to quantum dots for intraoperative near-infrared fluorescent sentinel lymph node mapping. *Mol Imaging.* 2005;4:172–81.
37. Bhushan KR, Tanaka E, Frangioni JV. Synthesis of conjugatable bisphosphonates for molecular imaging of large animals. *Angew Chem Int Ed Engl.* 2007;46:7969–71.
38. Soltesz EG, Laurence RG, De Grand AM, Cohn LH, Mihaljevic T, Frangioni JV. Image-guided quantification of cardioplegia delivery during cardiac surgery. *Heart Surg Forum.* 2007;10: E381–6.
39. Tanaka E, Choi HS, Humblet V, Ohnishi S, Laurence RG, Frangioni JV. Real-time intraoperative assessment of the extrahepatic bile ducts in rats and pigs using invisible near-infrared fluorescent light. *Surgery.* 2008;144:39–48.
40. Knapp DW, Adams LG, Degrand AM, et al. Sentinel lymph node mapping of invasive urinary bladder cancer in animal models using invisible light. *Eur Urol.* 2007;52:1700–8.
41. Flaumenhaft R, Tanaka E, Graham GJ, et al. Localization and quantification of platelet-rich thrombi in large blood vessels with near-infrared fluorescence imaging. *Circulation.* 2007;115:84–93.
42. Tanaka E, Chen FY, Flaumenhaft R, Graham GJ, Laurence RG, Frangioni JV. Real-time assessment of cardiac perfusion, coronary angiography, and acute intravascular thrombi using dual-channel near-infrared fluorescence imaging. *J Thorac Cardiovasc Surg.* 2009 (in press).
43. Paladini G, Azar FS. An extensible imaging platform for optical imaging applications. SPIE Photonics West - Multimodal Biomedical Imaging IV (Session 2), Proceedings of SPIE 2009;7171.
44. Zakaria S, Hoskin TL, Degnim AC. Safety and technical success of methylene blue dye for lymphatic mapping in breast cancer. *Am J Surg.* 2008;196:228–33.